Int. J. Environ. Sci. Technol. (2017) 14:2423–2434
DOI 10.1007/s13762-017-1328-9

ORIGINAL PAPER

Recovery of Cr(VI) by using a novel calix[4]arene polymeric membrane with modified graphene quantum dots

C. Onaç[1] · A. Kaya[1] · H. K. Alpoğuz[1] · M. L. Yola[2] · S. Eriskin[1] · N. Atar[4] · İ. Şener[3]

Received: 7 April 2016 / Revised: 8 March 2017 / Accepted: 21 April 2017 / Published online: 2 May 2017

Abstract In this report, the recovery of Cr(VI) from chrome plating water by using a novel calix[4]arene-functionalized graphene quantum dots (GQDs) involved polymer inclusion membrane was investigated. The polymeric membrane supported by GQDs was characterized by using Fourier transform infrared (FTIR), scanning electron microscopy (SEM) and atomic force microscopy (AFM). The SEM and AFM results clearly show that there are much larger visible pores on the membrane surface after modification of polymer inclusion membrane with GQDs and the micropores in the membrane surface were vanished and performed with GQDs after modification of membrane. The transport efficiency of chromium was found to be 97.23% through the modified membrane from 0.1 M HCl as donor phase to pH 5 as an acceptor phase. The system is available for long-term usage. The highly selective and mechanical strength of membrane is developed by adding GQDs. Modified membrane exhibits significant stability and selectivity, and the system is used for the real samples.

Editorial responsibility: M. Abbaspour.

✉ N. Atar
necipatar@gmail.com

[1] Department of Chemistry, Pamukkale University, Denizli, Turkey

[2] Department of Metallurgical and Materials Engineering, Sinop University, Sinop, Turkey

[3] Department of Food Engineering, Faculty of Engineering and Architecture, Kastamonu University, 37200 Kastamonu, Turkey

[4] Department of Chemical Engineering, Pamukkale University, Denizli, Turkey

Graphical Abstract

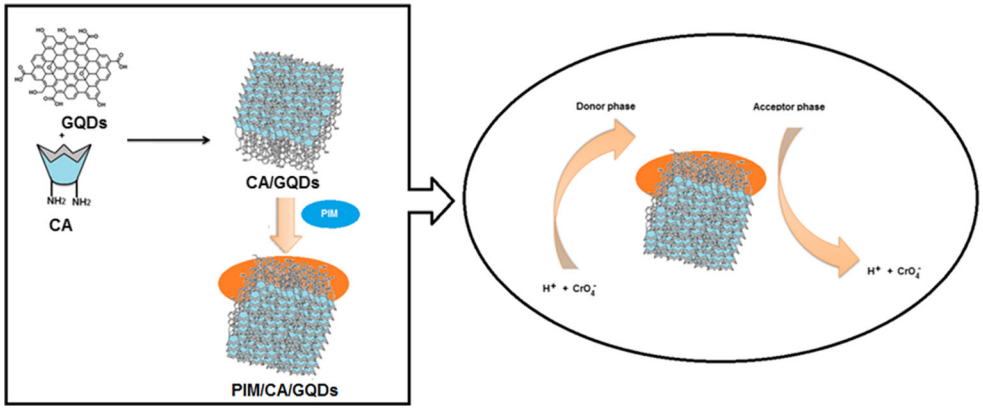

Keywords Calix[4]arene · Cr(VI) · Graphene quantum dots · Polymer inclusion membrane

Introduction

The rapid population growth, industrial activities global warming, increasing in drought and excessive consumption cause rapid and increased consumption of fresh water resources on a global scale. The protection of water resources has become of critical importance for next generations due to the increase in water demand by the rapid population growth, shortage of water resources, pollution issues, the excessive usage of water by industrial and agricultural activities (Atar and Olgun 2009; Atar et al. 2012).

The separation of toxic metals is significant by nano-reinforced membranes. The technology of membrane suggests affective method in comparison with many separations. There are crucial parameters in terms of membrane's usage, selectivity and price. These parameters are useful and affordable methods for treatment (Garcia-Rodríguez et al. 2015). Because of these problems, more energy use is necessary during operating processes. In addition, membrane cleaning is difficult. To remove these problems, the membrane performance and efficiency are improved. The modification of the membranes with novel materials is attractive topic on membrane technology (Nash et al. 2015).

Graphene quantum dots (GQDs) are smaller than 100 nm. They have crucial functions such as large surface area and high conductivity (Sanghavi et al. 2013, 2014; Kalambate et al. 2015; Sanghavi et al. 2015a, b; Atar et al. 2016; Sanghavi et al. 2016).

In studies, transport of metal ions is performed through ion exchange or complexing substances (Duffey et al. 1978; Kolev et al. 1997; Aguilar et al. 2001; Kozlowski and Walkowiak 2005; Scindia et al. 2005). The various reagents such as chelate and neutral solutions were utilized in the polymer inclusion membrane (PIM) (Kaya et al. 2013, 2014, 2016). The compounds with least nine members and three heterocyclics are considered as macrocyclic compounds. In recent years, after the crown ethers and cyclodextrins which are a natural glucose, oligomer calixarenes (CA) have emerged which is a phenol–formaldehyde oligomer in cyclic structure. These compounds can be synthesized and easily functionalized from other macrocyclic compounds.

In macrocyclic compounds of supramolecular chemistry, calixarenes are still the most popular compounds in the last years (Shedge et al. 2005). Calix[4]arenes are macrocyclic molecules. They complex with many molecules such as cations, anions and neutral compounds, and they have spaces to locate the host–guest molecules. Scheme 1 presents the interactions of calix[4]arene amine with chromate anions in acidic media.

Chromium is contaminant to soil and water. It has two oxidation states as Cr(III) and Cr(VI). Cr(VI) is toxic in environment. Owing to its resistance, it is essential in industries. It is a very hard metal that protects brightness and is not oxidized. Due to its hardness, it is used in the steel industry and business machines.

The plating of chrome is the formation of thin layer of chromium on any objects. The bath of chromium is a

mixture of chromium trioxide and sulfuric acid. Cr(VI) is one of the most toxic metals for human health. Cr(VI) has the high toxicity. Because of this, Cr(VI) should be controlled (Kaya et al. 2013). The experimental research study was performed in March 2015–December 2015 in the Chemical Research Laboratory of Pamukkale University of Science and Art Faculty at Denizli, Turkey.

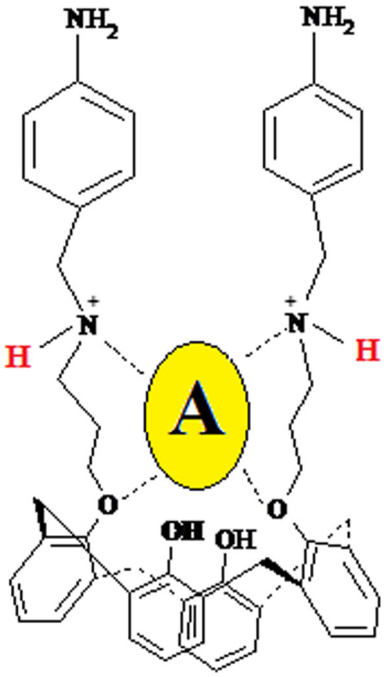

Scheme 1 Proposed interactions of a novel calix[4]arene carrier with chromate anions (*A* chromate anions)

In the report, the synthesis and characterization of 25,27-bis[2-*N*-(4-amiobenzyl)aminopropoxy]-26,28-dihydroxycalix[4]arene as a carrier of Cr(VI) were reported. The reaction scheme for the synthesis of calix[4]arene derivative is shown in Scheme 2.

Materials and methods

The whole chemicals were purchased from Sigma-Aldrich. Melting points were calculated by using Stuart smp 30 melting point apparatus (UK). Organic compounds such as cellulose tri acetate (CTA) (M_n = 72.000–74.000), 2-nitrophenyloctyl ether (2-NPOE), dichloromethane and *N*-(3-dimethylaminopropyl)-*N*′-ethylcarbodiimidehydrochloride (EDC) were used.

Synthesis

5,11,17,23-Tetra-tert-buthylcalix[4]arene (1), 25,26,27,28-tetrahydroxycalix[4]arene (2), 25,27-bis(3-bromopropoxy)-26,28-dihydroxycalix[4]arene (3) were synthesized in the previously literature procedure (Gutsche et al. 1986; Gutsche and Iqbal 1990; Li et al. 1999).

Synthesis of 25,27-bis[2-*N*-(4-amiobenzyl)amino-propoxy]-26,28-dihydroxycalix[4]arene (4)

25,27-Bis(3-bromopropoxy)-26,28-dihydroxycalix[4]arene (0.150 mmol) was dissolved in dimethyformamide (DMF)

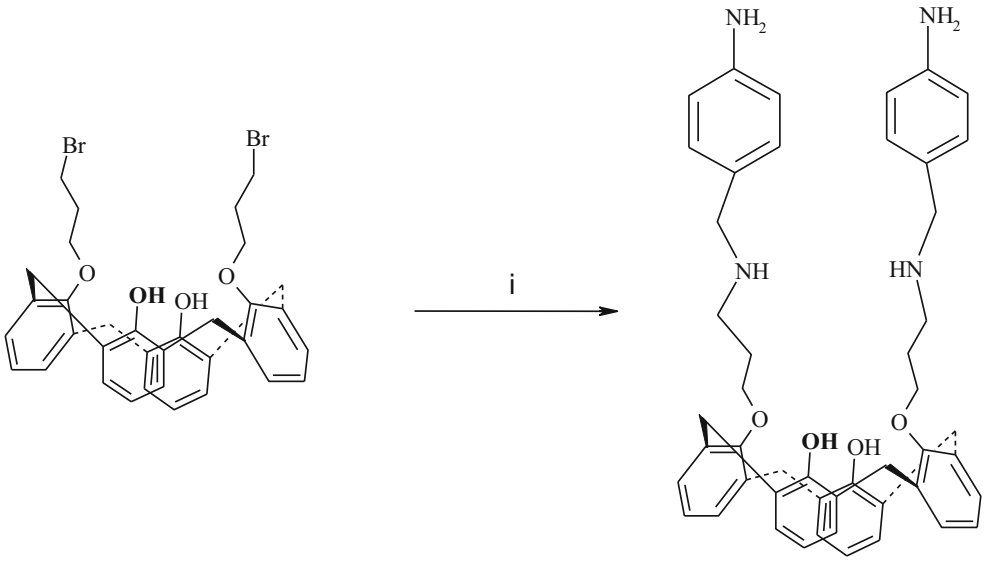

Scheme 2 Synthesis of calix[4]arene derivative (i) 4-aminobenzylamine, K_2CO_3, DMF

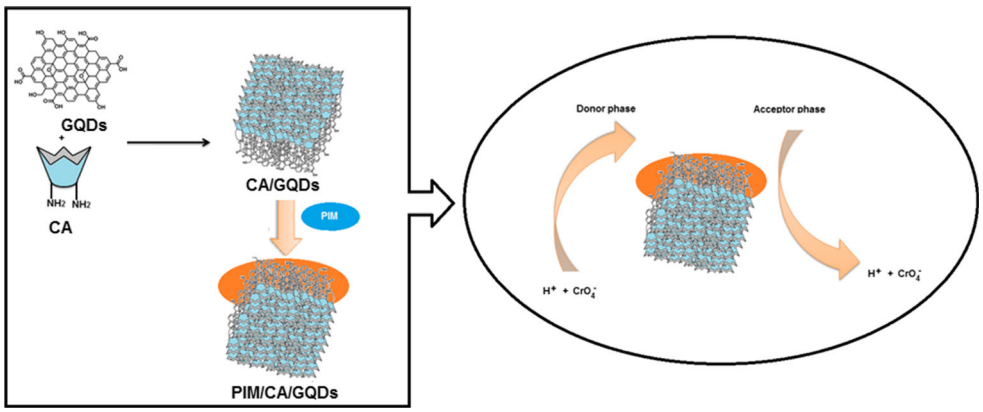

Scheme 3 The schematic representation of the formation of PIM/CA/GQDs

(100 mL). K_2CO_3 (1.5 mmol) was added to this solution with vigorous stirring. A solution of 4-aminobenzylamine (0.300 mmol) in DMF was added, and the reaction mixture was stirred for 48 h at room temperature. Then, the mixture was filtered off. After that, concentrated dichloromethane CH_2Cl_2 (30 mL) was added into the mixture. The organic phase was dried over anhydrous $MgSO_4$ and concentrated and crystallized from DMF–H_2O mixture. Yield 0.084 g (75%); mp: 152–154 °C. FTIR ν_{max} (cm^{-1}): 3350 (–OH), 3224 (–NH and $–NH_2$), 3059 and 3018 (Ar–H), 2920 and 2866 (aliphatic C–H), 1196 (C–O). **^{1}H-NMR** (400 MHz, $CDCl_3$) δ (ppm): 2.13 (m, 4H,), 3.47 (d, 4H, Ar**CH_2**Ar), 3.65 (t, 4H), 3.78 (s, 4H,), 4.15 (d, 4H, Ar**CH_2**Ar), 4.28 (t, 4H), 5.15 ppm (s, 4H, –N**H_2**)5.61 ppm (s, 2H, –N**H**), 6.68–7.32 ppm (m, 20H, Ar**H**), 7.68 (s, 2H, calix-**OH**). Anal. Cal. for $C_{48}H_{52}N_4O_4$; C: 77%; H: 6.95%; N: 7.49%. Found: C: 77.02%; H: 6.96%; N: 4.47%.

Synthesis of GQDs

Graphene oxide and GQDs were synthesized according to our previous reports (Yola et al. 2014) (Atar et al. 2015a, b, c; Gupta et al. 2015; Yola et al. 2015). For the surface activation of carboxylate groups of GQDs, the GQDs suspension was interacted with 0.2 M EDC solution for 8 h. After that, 1.0 mM calix[4]arene was mixed with the activated GQDs suspension at a 1:1 volume ratio and kept stirring for 2 h (CA/GQDs) (Gupta et al. 2013a, b; Atar et al. 2015a, b, c). The membrane was developed according to the methods (Sap et al. 2012; Kaya et al. 2013; Onac et al. 2013; Kaya et al. 2014). The schematic formation of PIM/CA/GQDs is shown in Scheme 3.

Addition of GQDs into the base polymer improves the structure. We tried to investigate PIM behaviors in the presence of GQD and understand how it affects PIM structural properties. GQDs go into the polymer structure. Therefore, if possible, it is recommended that the PIM experiments should be carried out preferably using modified membrane with GQDs.

The studies of transport

The transport experiments were carried out in a permeation cell (Kaya et al. 2013; Onac et al. 2013; Kaya et al. 2014); $0.2.0 \times 10^{-4}$ M $K_2Cr_2O_7$ in 0.1 M HCl was used as a donor phase. The acceptor phase was adjusted at pH 5.

Cr(VI) amount was obtained in an acidic media (Castillo et al. 2002; Kaya et al. 2013, 2014). The rate constant (k) and permeability coefficient (P) were evaluated by a first order (Pedersen 1968; Danesi 1984; Kozlowski and Walkowiak 2002; Bayrakci et al. 2009).

The relationship between ln (C/C_i) and time was linear (r^2) 0.9588–0.9937.

We calculated the recovery factor (RF) with Eq. (1) for Cr(VI) removal

$$\mathrm{RF} = \frac{C_\mathrm{i} - C}{C_\mathrm{i}} \times 100\,\% \qquad (1)$$

C_i is the initial amount of Cr(VI) and C is the amount of Cr(VI) at given time.

Characterization of the PIM/CA/GQDs membrane

The membrane morphology is one the most crucial aspects of PIMs studies. FTIR is the method to illuminate the membrane structure. Perkin-Elmer Spectrum Two DTGS spectrum software was used to carryout FTIR measurements between 4000 and 450 cm^{-1}. There are no

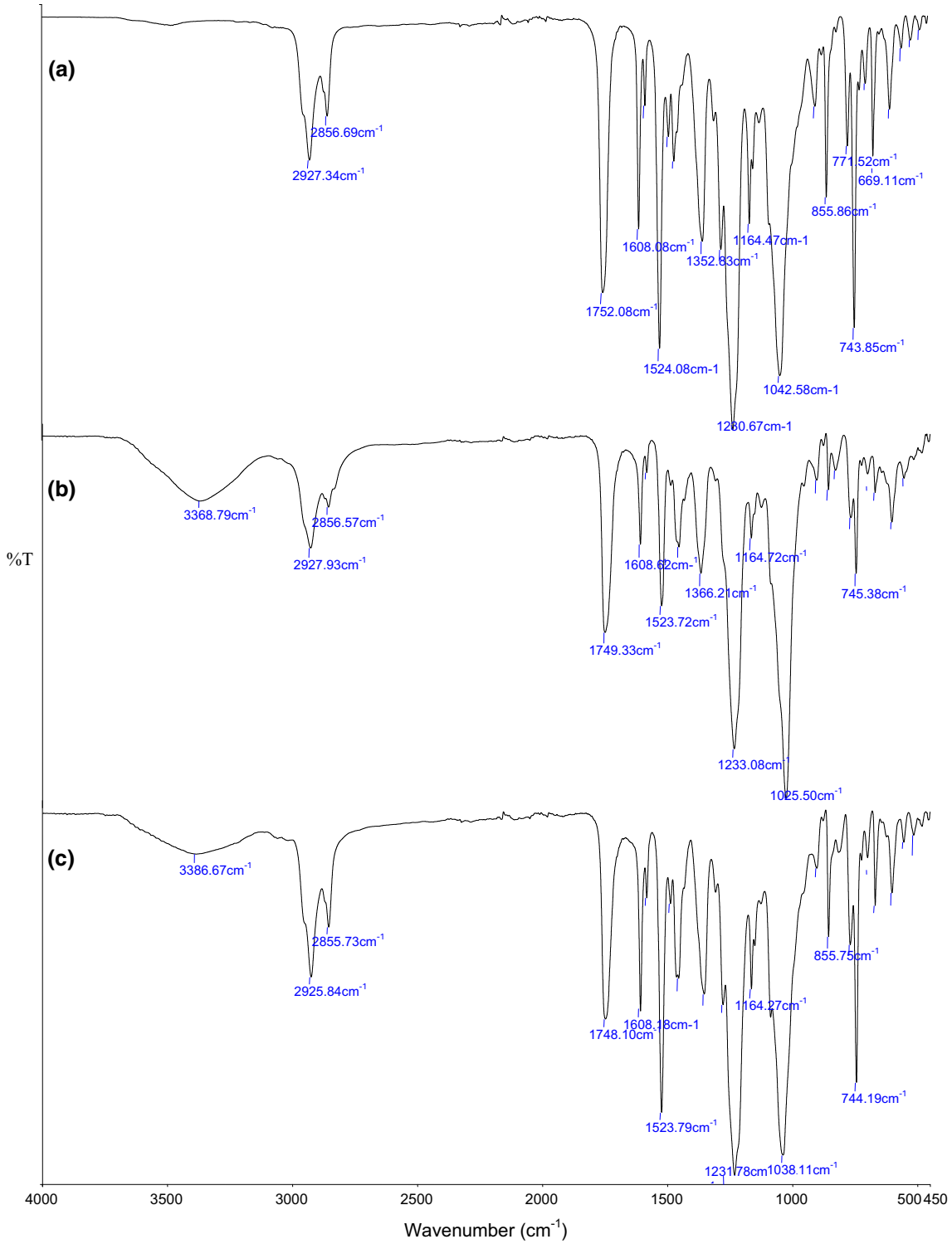

Fig. 1 **a** FTIR spectra of blank membrane, **b** PIM + calix[4]arene carrier, **c** PIM/CA/GQDs

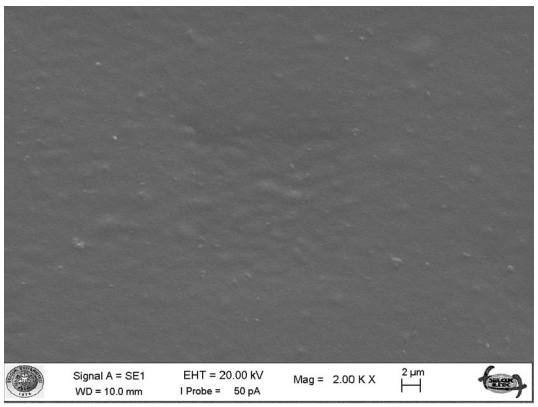

(a)

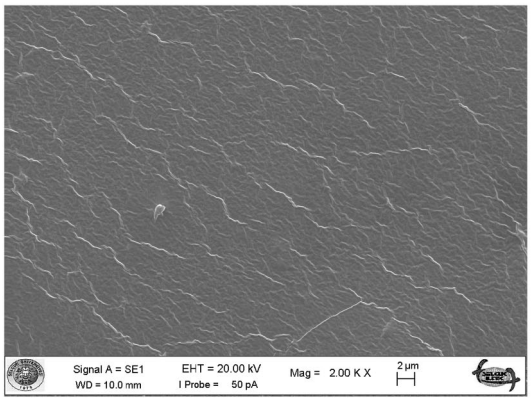

(b)

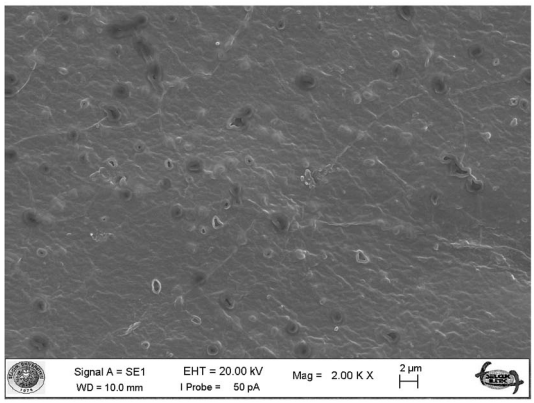

(c)

Fig. 2 **a** SEM surface photographs of blank membrane, **b** SEM surface photographs of PIM/CA/GQDs, **c** SEM surface photographs of PIM/CA/GQDs

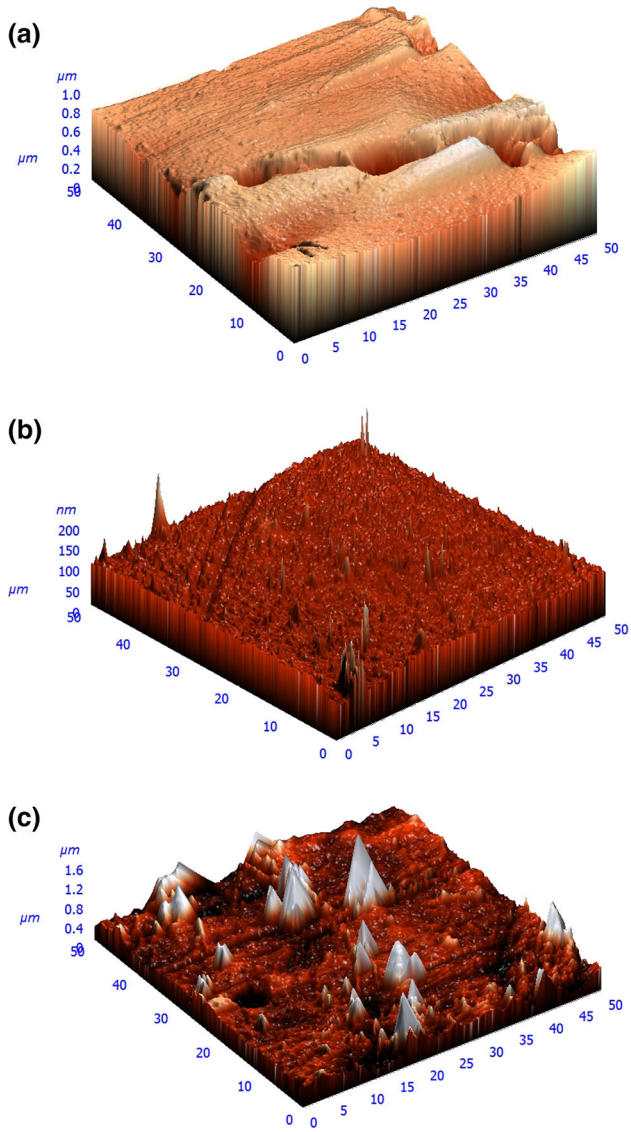

Fig. 3 **a**Three-dimensional figure of AFM for a blank membrane (CTA + 2-NPOE), **b** three-dimensional figure of AFM for PIM with calix[4]arene, **c** three-dimensional figure of AFM for PIM/CA/GQDs

intermolecular covalent bonds in a stable membrane. The forces of intermolecular determinate the membrane structure (Nghiem et al. 2006). Figure 1 presents the measurement of the FTIR spectrum of blank membrane (Fig. 1a), PIM with carrier (Fig. 1b), PIM/CA/GQDs with carrier (Fig. 1c), respectively. As we mentioned before, in the section of synthesis of calix[4]arene derivative, there were absorption bands at around 3350 cm^{-1} which were related to stretching vibrations of O–H groups (Stuart 2004). In Fig. 1b (PIM + carrier), the absorption bands of O–H groups were deformed and the situation showed that calix[4]arene carrier was bonded to PIM (CTA + 2-NPOE) via O–H groups. In addition, the absorption bands at around 3368 cm^{-1} are corresponded to -NH and NH_2 groups which were existed after adding calix[4]arene carrier to the blank membrane. This band is corresponded to

Table 1 The effect of the type of plasticizers

Plasticizer type	εr	η (cP)	$K \times 10^4$ (s^{-1})	$P \times 10^6$ (m/s)	RF (%)
2-Nitrophenylpentyl ether (2-NPPE)	24	7.58	1.299	6.438	97.44
2-Nitrophenyloctyl ether (2-NPOE)	24	12.35	1.983	9.828	99.56
Tris (2-ethylhexyl) phosphate (T2EHP)	4.8	13.1	0.587	2.909	82.00
Tris (2-butoxy ethyl) phosphate (TBEP)	4.2	13.8	0.062	0.307	18.81

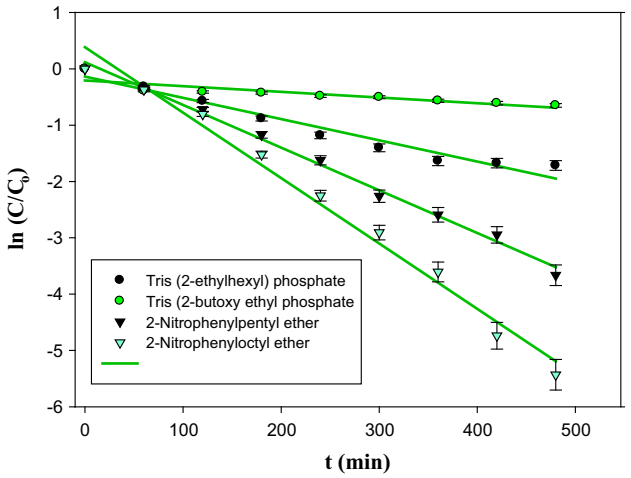

Fig. 4 ln(C/Co) values versus time with four different plasticizer types: donor phase: 2×10^{-4} M $K_2Cr_2O_7$ in 1 M HCl, membrane composite: 2 mL plasticizer/1 g CTA, graphene quantum dots (1% w/w), 0.6 M calix[4]arene, acceptor phase: pH 5 acetic acid/ammonium acetate buffer, stirring rate: 500 rpm

the presence of calix[4]arene carrier in the membrane, and calix[4]arene carrier was bonded to membrane via O–H groups. In Fig. 1c, the absorption bands of -NH and NH_2 were deformed (3386 cm^{-1}). This situation demonstrated that GQDs were bonded to the PIM + carrier via –NH and NH_2 groups.

The SEM images of blank membrane (Fig. 2a), PIM + carrier (Fig. 2b) and PIM/CA/GQDs (Fig. 2c) were obtained. The magnification of all SEM images was 2.000× and cross section of a 2 μm thick. As we can understand the FTIR spectrums of the blank membrane, PIM + calix[4]arene, PIM/CA/GQDs, there are similar functional groups in the spectrum. The surface of Fig. 2a is a smooth when we compared with the other two pictures of Fig. 2b, c. After bonding the calix[4]-arene to the membrane, the surface became rougher (Fig. 2b). Figure 2b is a SEM image of unmodified PIM (PIM + calix[4]arene), when we compared with Fig. 2c, which is a SEM image of PIM/CA/GQDs, the highly porous polymer matrix is shown in Fig. 2c. The roughness was vanished, and the dark and deep pores which belong to GQDs are clearly visible after modification of PIM with GQDs (Fig. 2c). The modification of PIM with GQDs resulted in fibrous structure of polymer matrix (Fig. 2c).

AFM is commonly used to understand the surface morphology. The samples were installed on a sample holder. AFM images of membranes were taken in three-dimensional format of 50 μm × 50 μm^2 sample area. Figure 3 shows the AFM pictures of blank membrane, PIM/CA and PIM/CA/GQDs. The surface of blank membrane picture is quite smooth. The difference between Fig. 3a and according to Fig. 3b, the pores become larger and more visible after adding calix[4]arene to the membrane. When we compared the pictures of Fig. 3b, c, the difference between the two pictures can easily noticeable. There are much larger visible pores on the membrane surface after modification of PIM with GQDs. GQDs are into the polymer matrix and reinforced the properties of membrane mechanical.

Roughness of PIM/CA/GQDs surface was also increased. The values of surface deepness for blank membrane and PIM/CA/GQDs are 60.30 ± 1.30 and 68.47 ± 1.25 nm, respectively. According to the results, PIM surface is formed with GQDs.

Table 2 The effect of the amount of plasticizers

Amount of 2-NPOE (2-NPOE/1 g CTA) (mL)	$K \times 10^4$ (s^{-1})	$P \times 10^6$ (m/s)	$J \times 10^6$ (mol/m^2 s)	$D \times 10^{10}$ (m^2/s)	RF (%)
1.50	1.241	6.150	1.230	3.018	97.81
1.75	1.329	6.586	1.317	3.250	97.25
2.00	1.983	9.828	1.966	4.739	99.56
2.25	1.300	6.443	1.289	3.107	99.55
2.50	1.120	5.551	1.110	2.776	95.93

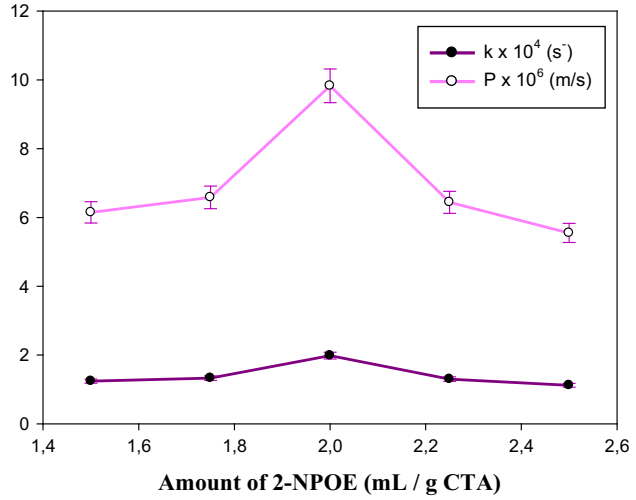

Fig. 5 Different amounts of plasticizer versus kinetic results (k, P) for Cr(VI) transport: donor phase: 2×10^{-4} M $K_2Cr_2O_7$ in 1 M HCl, membrane composite: 1.50–2.50 mL 2-NPOE/1 g CTA, graphene quantum dots (1% w/w), 0.6 M calix[4]arene, acceptor phase: pH 5 acetic acid/ammonium acetate buffer, stirring rate: 500 rpm

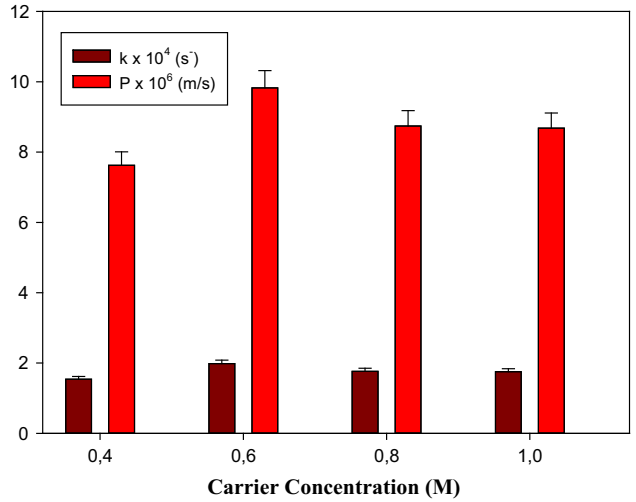

Fig. 6 Different carrier concentration values versus kinetic results (k, P) for Cr(VI) transport: donor phase: 2×10^{-4} $MK_2Cr_2O_7$ in 1 M HCl, acceptor phase: pH 5 acetic acid/ammonium acetate buffer, membrane composite 2 mL 2-NPOE/1 g CTA, with different calix[4]arene carrier concentrations, graphene quantum dots (1% w/w)

Results and discussion

The effect of plasticizer type

The rigidity is not conducive in the polymer. Hence, the plasticizers are utilized. The plasticizers can increase the distance between the polymer molecules or polar groups (Nghiem et al. 2006). The balance between the polar and apolar parts of the plasticizer molecules is a significant element in physicochemical properties of plasticizers. Suguira (1992) prepared PIM including in polyoxyethylene alkyl ethers as a plasticizer. This plasticizer includes different alkyl chain lengths and different number of polar oxyethylene groups. They presented that the increase in alkyl chain lengths resulted in more hydrophobic property and the viscose plasticizers suppress the polar properties of plasticizer. Unlike it, the increase in the number of the polar groups of plasticizer decreased viscosity and increased hydrophility of plasticizer (Sugiura 1992).

We carried out the experiments with four different plasticizers: 2-NPOE, 2-nitrophenylpentyl ether (2-NPPE), tris (2-ethylhexyl) phosphate (T2EHP) and tris (2-butoxy ethyl) phosphate (TBEP). The dielectric constant (polarity) and the viscosity of the plasticizer are present in plasticizer type. As shown in Table 1, the best kinetic result was taken with 2-NPPE and 2-NPOE. The ion pairs are diffused easily between the carrier and the active areas of plasticizers (Fig. 4). 2-NPOE was used as a plasticizer owing to its low cost.

The amount of plasticizer in the membrane phase

The low plasticizer concentration is called as effect of anti-plasticizer and is not desirable to form hard and brittle membrane. The minimum concentration of plasticizer changes depending on both type of plasticizer and polymer. The excessive concentration of plasticizers is an undesired condition because it constitutes an additional barrier on the membrane surface to transport of metal ions and makes difficult the transport process on membrane/aqueous. The transported metal concentration depends on the compatibility between the base polymer and plasticizer, and it would be more transition in level of convenient concentration. In addition, the excessive concentration significantly reduces the mechanic force of membrane and this situation makes the membrane unusable in practice. In some of PIM studies, it is observed that increasing in plasticizer concentration increases metal-ion transport. But, when wide concentration range of optimum plasticizer occurs, maximum metal-ion flux is achieved. As a result, it is really important to study the plasticizer concentration on the transport process.

In this study, we prepared the membrane with five different amounts of plasticizer (2-NPOE) with a constant concentration of carrier and base polymer (CTA). The kinetic results are given in Table 2.

All kinetic results increase from 1.50 to 2.00 mL until the limited value is reached. After 2.00 mL amount of plasticizer, the kinetic results begin to decrease (Table 2; Fig. 5). The increase in the amount of plasticizer

Table 3 The effect of the acceptor phase pH

Acceptor phase pH	$K \times 10^4$ (s^{-1})	$P \times 10^6$ (m/s)	$J \times 10^6$ (mol/m^2 s)	$D \times 10^{10}$ (m^2/s)	RF (%)
4	0.969	4.802	0.960	2.466	93.44
4.5	1.693	8.390	1.678	4.070	98.94
5	1.983	9.828	1.966	4.739	99.56
6	1.747	8.658	1.732	4.175	97.46

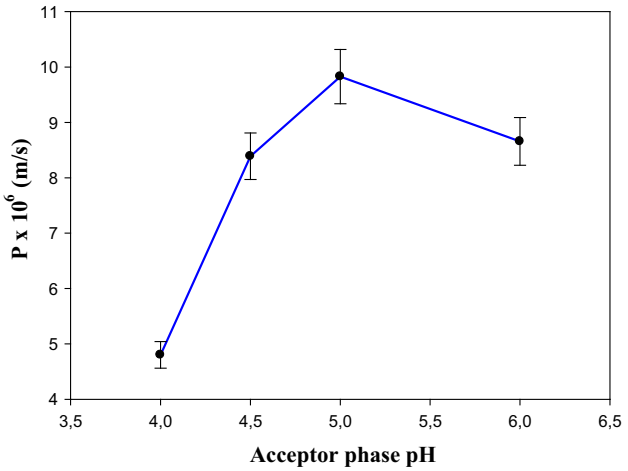

Fig. 7 Acceptor phase pH values versus permeability (*P*) for Cr(VI) transport: donor phase: 2×10^{-4} M $K_2Cr_2O_7$ in 1 M HCl, membrane composite: 2 mL 2-NPOE/1 g CTA, graphene quantum dots (1% w/w), 0.6 M calix[4]arene carrier, acceptor phase: pH 4–6 acetic acid/ammonium acetate buffer, stirring rate: 500 rpm

Table 4 Initial concentration of chrome plating bath water and RF (%) values of transport studies

Metal ions in chrome plating bath water	Initial concentration (ppm)	RF (%)
Cr(VI)	15.6	97.23
Fe(III)	0.28	<1
Ni(II)	1.62	<1
Pb(II)	0.10	<1

constitutes an additional barrier on the membrane surface, so transport of Cr(VI) metal cation begins to decrease after the maximum value.

The effect of carrier concentration

In the studies of PIM, the transport is performed by carrier which is ion-exchanger or complexing agent and it is important to maximize the membrane fluxes in terms of the transport efficiency, permeability and selectivity. The transport process can be extremely affected by amount and physicochemical properties of carrier. In addition, the chemical structure of membrane phase should be in harmony with donor and acceptor phases to achieve the transport process. PIM researches have studied chelate, all macrocyclic and macromolecular compounds. In PIM studies, the type of carrier is significant for the transport, but excessive amounts of carrier can be concluded assemblage in membrane phase and transudation to acceptor and donor phases. Subsequently, we investigate the effect of carrier concentration in this study. The effect of carrier concentration was studied under four concentrations (0.4, 0.6, 0.8 and 1 M). There are recovery factor RF (%) values in Fig. 6. RF (%) values increase with the increasing in Cr(VI) concentration, but RF (%) values began to decrease after 0.6 M carrier concentration. The reason of this phenomenon is related to membrane viscosity and thickness. The increasing in carrier concentration increases the membrane viscosity. The high membrane viscosity delimitates the diffusion of Cr(VI)–carrier complex that occurs in the interface of donor/membrane phase. The excessive carrier concentration accumulates on the membrane surface at the same time and causes the blocking of membrane pores.

The influence of pH

The different pH values (4, 4.5, 5 and 6) were tried for the effect of the pH. $HCrO_4^-$ ions are dominant in acidic

Table 5 Comparison of PIM, PIM/CA and PIM/GQDs transport studies for Cr(VI)

Membrane structure	$K \times 10^4$ (s^{-1})	$P \times 10^6$ (m/s)	$J \times 10^6$ (mol/m^2 s)	$D \times 10^{10}$ (m^2/s)	RF (%)
PIM	0.106	0.525	0.105	2.057	12.25
PIM/CA	1.756	8.703	1.741	4.579	91.23
PIM/GQDs	1.983	9.828	1.966	4.739	99.56

conditions. Eighty percentage of total Cr(VI) bi-2-is existed as $HCrO_4^-$ in the range of 0–5. The rest 20% as $(Cr_2O_7)^{2-}$ chromates. Hundred percentage of Cr(VI) exists in the form of $(Cr_2O_7)^{2-}$ in the range of 7.5–14. The three species coexist in various proportions in the range of 5.0–7.5. It is observed that Cr(VI) has the most negative charge per species at pH values over 7.5. Due to deprotonation of the calix[4]arene at higher pH values, a decrease in the transport rate was seen. The complexation occurs in acidic conditions. The kinetic results of Cr(VI) transport are shown in Table 3. In low pH values, Cr(VI) ions diffuse to the carrier of the membrane and decompose from the carrier in high pH values. Subsequently, the pH of acceptor phase is higher than the pH of donor phase. As shown in Fig. 7, the optimum permeability results were achieved in pH 5.

Selectivity of PIM/CA/GQDs against Cr(VI)

The complex between the metal ion and the calix[4]arene with two amino groups facilitates the transport (Nghiem et al. 2006). The experiments were performed in the presence of Fe(III), Ni(II) and Pb(II) metals. The real sample was diluted 8000 times to remove Cr(VI). The contents of the diluted chrome plating are given in Table 4. After 8 h, Cr(VI) was transported with a recovery factor of 97.23%. So, the calix[4]arene derivative showed a good selectivity. We can say that the studies of PIM/CA/GQDs are practical for many applications.

Comparison of PIM and PIM/GQDs transport studies

Generally, there is no crucial comment for membrane life in PIM investigations (Nghiem et al. 2006). The studies are performed to increase membrane life by adding base polymers or restoring conditions. The membrane within organic additives shows excellent membrane performance. In the report, the modification of membrane by GQDs provides better mechanical properties in terms of the structure and performance. For this purpose, PIM and PIM/CA/GQDs transport studies were achieved. Table 5 presents the kinetic results of PIM and PIM/CA/GQDs. According to the results, PIM/CA/GQDs cause better k, P, diffusion coefficient (D), flux (J) and RF (%) values than PIM.

Conclusion

In the report, the modification of membrane is very crucial for high permeability, porous structure and high selectivity. Hence, improved mechanical properties and reproducibility can be provided. PIM/CA/GQDs show good stability and selectivity and can be used with high recovery. The modification of membrane by GQDs with the pores on the membrane surface shows good mechanical properties. We can say that the experiments of PIM can be performed by using GQDs.

Acknowledgments This work is supported by the Scientific Research Projects (BAP) of Pamukkale University, Denizli, Turkey (2015FBE009).

List of symbols

PIM	Polymer inclusion membrane
GQDs	Graphene quantum dots
CA	Calix[4]arene
2-NPOE	2-Nitrophenlyoctyl ether
EDC	*N*-(3-Dimethylaminopropyl)-*N*′-ethylcarbodiimide hydrochloride
TMS	Tetramethylsilane
DMF	Dimethyl formamide
CTA	Cellulose triacetate
PVC	Polyvinyl chloride
SEM	Scanning electron microscopy
AFM	Atomic force microscopy
FTIR	Fourier transform infrared spectroscopy
1H-NMR	Nuclear magnetic resonance
(δ)	Chemical shifts
k	Rate constant
P	Permeability
J	Flux
D	Diffusion coefficient
RF	Recovery factor

References

Aguilar JC, Sánchez-Castellanos M, de San Miguel ER, de Gyves M (2001) Cd(II) and Pb(II) extraction and transport modeling in SLM and PIM systems using Kelex 100 as carrier. J Membr Sci 190(1):107–118. doi:10.1016/S0376-7388(01)00433-1

Atar N, Olgun A (2009) Removal of basic and acid dyes from aqueous solutions by a waste containing boron impurity. Desalination 249(1):109–115. doi:10.1016/j.desal.2008.12.045

Atar N, Olgun A, Wang S (2012) Adsorption of cadmium(II) and zinc(II) on boron enrichment process waste in aqueous solutions: batch and fixed-bed system studies. Chem Eng J 192:1–7. doi:10.1016/j.cej.2012.03.067

Atar N, Eren T, Demirdögen B, Yola ML, Çağlayan MO (2015a) Silver, gold, and silver@gold nanoparticle-anchored L-cysteine-functionalized reduced graphene oxide as electrocatalyst for methanol oxidation. Ionics 21(8):2285–2293. doi:10.1007/s11581-015-1395-1

Atar N, Eren T, Yola ML, Gerengi H, Wang S (2015b) Fe@Ag nanoparticles decorated reduced graphene oxide as ultrahigh capacity anode material for lithium-ion battery. DOI, Ionics. doi:10.1007/s11581-015-1520-1

Atar N, Eren T, Yola ML, Karimi-Maleh H, Demirdögen B (2015c) Magnetic iron oxide and iron oxide@gold nanoparticle anchored nitrogen and sulfur-functionalized reduced graphene oxide

electrocatalyst for methanol oxidation. RSC Adv 5(33):26402–26409. doi:10.1039/c5ra03735b

Atar N, Yola ML, Eren T (2016) Sensitive determination of citrinin based on molecular imprinted electrochemical sensor. Appl Surf Sci 362:315–322. doi:10.1016/j.apsusc.2015.11.222

Bayrakci M, Ertul S, Sahin O, Yilmaz M (2009) Synthesis of two new p-tert-butylcalix[4]arene β-ketoimin derivatives for extraction of dichromate anion. J Incl Phenom Macrocycl Chem 63(3–4):241–247. doi:10.1007/s10847-008-9513-6

Castillo E, Granados M, Cortina JL (2002) Chemically facilitated chromium(VI) transport throughout an anion-exchange membrane: application to an optical sensor for chromium(VI) monitoring. J Chromatogr A 963(1–2):205–211. doi:10.1016/S0021-9673(02)00362-X

Danesi PR (1984) Separation of metal species by supported liquid membranes. Sep Sci Technol 19(11–12):857–894

Duffey ME, Evans DF, Cussler EL (1978) Simultaneous diffusion of ions and ion pairs across liquid membranes. J Membr Sci 3(1):1–14. doi:10.1016/S0376-7388(00)80407-X

Garcia-Rodríguez A, Matamoros V, Kolev SD, Fontàs C (2015) Development of a polymer inclusion membrane (PIM) for the preconcentration of antibiotics in environmental water samples. J Membr Sci 492:32–39. doi:10.1016/j.memsci.2015.05.037

Gupta VK, Atar N, Yola ML, Eryilmaz M, Torul H, Tamer U, Boyaci TH, Üstündağ Z (2013a) A novel glucose biosensor platform based on Ag@AuNPs modified graphene oxide nanocomposite and SERS application. J Colloid Interface Sci 406:231–237. doi:10.1016/j.jcis.2013.06.007

Gupta VK, Yola ML, Qureshi MS, Solak AO, Atar N, Üstündağ Z (2013b) A novel impedimetric biosensor based on graphene oxide/gold nanoplatform for detection of DNA arrays. Sens Actuators B Chem 188:1201–1211. doi:10.1016/j.snb.2013.08.034

Gupta VK, Eren T, Atar N, Yola ML, Parlak C, Karimi-Maleh H (2015) $COFe_2O_4$@TiO_2 decorated reduced graphene oxide nanocomposite for photocatalytic degradation of chlorpyrifos. J Mol Liq 208:122–129. doi:10.1016/j.molliq.2015.04.032

Gutsche CD, Iqbal M (1990) Para-tert-butylcalix 4 arene. Org Synth 68:234–237

Gutsche CD, Iqbal M, Stewart D (1986) Calixarenes. 18. Synthesis procedures for p-tert-butylcalix[4]arene. J Org Chem 51(5):742–745

Kalambate PK, Sanghavi BJ, Karna SP, Srivastava AK (2015) Simultaneous voltammetric determination of paracetamol and domperidone based on a graphene/platinum nanoparticles/nafion composite modified glassy carbon electrode. Sens Actuators B Chem 213:285–294. doi:10.1016/j.snb.2015.02.090

Kaya A, Alpoguz HK, Yilmaz A (2013) Application of Cr(VI) transport through the polymer inclusion membrane with a new synthesized calix[4]arene derivative. Ind Eng Chem Res 52(15):5428–5436. doi:10.1021/ie303257w

Kaya A, Onac C, Surucu A, Karapinar E, Alpoguz HK, Tabakci B (2014) Preparation of CTA-based polymer inclusion membrane using calix[4]arene derivative as a carrier for Cr(VI) transport. J Incl Phenom Macrocycl Chem 79(1–2):103–111. doi:10.1007/s10847-013-0329-7

Kaya A, Onac C, Alpoguz HK, Yilmaz A, Atar N (2016) Removal of Cr(VI) through calixarene based polymer inclusion membrane from chrome plating bath water. Chem Eng J 283:141–149. doi:10.1016/j.cej.2015.07.052

Kolev SD, Argiropoulos G, Cattrall RW, Hamilton IC, Paimin R (1997) Mathematical modelling of membrane extraction of gold(III) from hydrochloric acid solutions. J Membr Sci 137(1–2):261–269. doi:10.1016/S0376-7388(97)00209-3

Kozlowski CA, Walkowiak W (2002) Removal of chromium(VI) from aqueous solutions by polymer inclusion membranes. Water Res 36(19):4870–4876. doi:10.1016/S0043-1354(02)00216-6

Kozlowski CA, Walkowiak W (2005) Applicability of liquid membranes in chromium(VI) transport with amines as ion carriers. J Membr Sci 266(1–2):143–150. doi:10.1016/j.memsci.2005.04.053

Li ZT, Ji GZ, Zhao CX, Yuan SD, Ding H, Huang C, Du AL, Wei M (1999) Self-assembling calix 4 arene 2 catenanes. Preorganization, conformation, selectivity, and efficiency. J Org Chem 64(10):3572–3584

Nash NH, Young TM, McGrail PT, Stanley WF (2015) Inclusion of a thermoplastic phase to improve impact and post-impact performances of carbon fibre reinforced thermosetting composites—a review. Mater Des 85:582–597. doi:10.1016/j.matdes.2015.07.001

Nghiem LD, Mornane P, Potter ID, Perera JM, Cattrall RW, Kolev SD (2006) Extraction and transport of metal ions and small organic compounds using polymer inclusion membranes (PIMS). J Membr Sci 281(1–2):7–41. doi:10.1016/j.memsci.2006.03.035

Onac C, Alpoguz HK, Akceylan E, Yilmaz M (2013) Facilitated transport of Cr(VI) through polymer inclusion membrane system containing calix[4]arene derivative as carrier agent. J Macromol Sci Part A Pure Appl Chem 50(10):1013–1021. doi:10.1080/10601325.2013.792205

Pedersen CJ (1968) Ionic complexes of macrocyclic polyethers. Fed Proc 27(6):1305–1309

Sanghavi BJ, Sitaula S, Griep MH, Karna SP, Ali MF, Swami NS (2013) Real-time electrochemical monitoring of adenosine triphosphate in the picomolar to micromolar range using graphene-modified electrodes. Anal Chem 85(17):8158–8165. doi:10.1021/ac4011205

Sanghavi BJ, Varhue W, Chávez JL, Chou CF, Swami NS (2014) Electrokinetic preconcentration and detection of neuropeptides at patterned graphene-modified electrodes in a nanochannel. Anal Chem 86(9):4120–4125. doi:10.1021/ac500155g

Sanghavi BJ, Gadhari NS, Kalambate PK, Karna SP, Srivastava AK (2015a) Potentiometric stripping analysis of arsenic using a graphene paste electrode modified with a thiacrown ether and gold nanoparticles. Microchim Acta 182(7–8):1473–1481. doi:10.1007/s00604-015-1470-3

Sanghavi BJ, Varhue W, Rohani A, Liao KT, Bazydlo LAL, Chou CF, Swami NS (2015b) Ultrafast immunoassays by coupling dielectrophoretic biomarker enrichment in nanoslit channel with electrochemical detection on graphene. Lab Chip Miniat Chem Biol 15(24):4563–4570. doi:10.1039/c5lc00840a

Sanghavi BJ, Moore JA, Chávez JL, Hagen JA, Kelley-Loughnane N, Chou CF, Swami NS (2016) Aptamer-functionalized nanoparticles for surface immobilization-free electrochemical detection of cortisol in a microfluidic device. Biosens Bioelectron 78:244–252. doi:10.1016/j.bios.2015.11.044

Sap A, Tabakci B, Yilmaz A (2012) Calix[4]arene-based Mannich and Schiff bases as versatile receptors for dichromate anion extraction: synthesis and comparative studies. Tetrahedron 68(42):8739–8745. doi:10.1016/j.tet.2012.08.015

Scindia YM, Pandey AK, Reddy AVR (2005) Coupled-diffusion transport of Cr(VI) across anion-exchange membranes prepared by physical and chemical immobilization methods. J Membr Sci 249(1–2):143–152. doi:10.1016/j.memsci.2004.10.015

Shedge AS, Lele AK, Wadgaonkar PP, Hourdet D, Perrin P, Chassenieux C, Badiger MV (2005) Hydrophobically modified poly(acrylic acid) using 3-pentadecylcyclohexylamine: synthesis and rheology. Macromol Chem Phys 206(4):464–472. doi:10.1002/macp.200400392

Stuart BH (2004) Infrared spectroscopy: fundamentals and applications. Wiley, Hoboken

Sugiura M (1992) Effect of polyoxyethylene normal-alkyl ethers on carrier-mediated transport of lanthanide ions through cellulose triacetate membranes. Sep Sci Technol 27(2):269–276. doi:10.1080/01496399208018878

Yola ML, Gupta VK, Eren T, Şen AE, Atar N (2014) A novel electro analytical nanosensor based on graphene oxide/silver nanoparticles for simultaneous determination of quercetin and morin. Electrochim Acta 120:204–211. doi:10.1016/j.electacta.2013.12.086

Yola ML, Atar N, Eren T, Karimi-Maleh H, Wang S (2015) Sensitive and selective determination of aqueous triclosan based on gold nanoparticles on polyoxometalate/reduced graphene oxide nanohybrid. RSC Adv 5(81):65953–65962. doi:10.1039/c5ra07443f